CT and MR Imaging of Hepatocellular Carcinoma

Nicolae Bolog[1], Gustav Andreisek[2], Irinel Oancea[1], Angelica Mangrau[1]

1) Phoenix Diagnostic Clinic, Bucharest, Romania; 2) University Hospital Zurich, Switzerland

Abstract

Hepatocellular carcinoma (HCC) is the fifth most common tumor in the world and the incidence is expected to increase in the future due to hepatitis viral infections and increasing cirrhosis incidence. The diagnosis of HCC is no longer based on biopsy especially in cases when curative treatment is possible. The imaging criteria are usually based on the vascular findings of HCC (e.g. early arterial uptake followed by washout in the portovenous and equilibrium phase). However, there are several limitations of the assessment of HCC by using only the vascular criteria. The use of tissue-specific contrast agents, including superparamagnetic iron oxides and hepatobiliary contrast agents, improves lesion detection and characterization. Therefore, an accurate diagnosis of HCC implies, at this moment, a combination of vascular and cellular information. This review focuses on the most important findings provided by the unenhanced and dynamic-enhanced CT and MR images regarding HCC evaluation. We also discuss the various imaging characteristics of HCC at MR imaging after the administration of tissue specific contrast agents.

Key-words

Liver – hepatocellular carcinoma – CT – MRI – contrast media.

Introduction

Hepatocellular carcinoma (HCC) is the fifth most common tumor in the world and its incidence is expected to increase in the future due to hepatitis viral infections and increased cirrhosis incidence [1, 2]. The diagnosis of HCC is no longer based on biopsy especially in the cases when curative treatment is possible. Approximately 30% of patients are candidates for curative treatments including liver transplantation, liver resection, and percutaneous interventions [1] with a 5-year survival rate between 40% and 75% [3]. Therefore, there is an increased expectation from radiologists in diagnosing HCC in early stages. The screening for HCC includes the alpha-fetoprotein level and ultrasonography. However, the sensitivity of ultrasound for HCC detection is low since small nodules can be missed in a cirrhotic liver. Computed tomography (CT) and magnetic resonance imaging (MRI) have a high sensitivity (55%-91%) and specificity (77%-96%) in diagnosing HCC [4]. According to the European Association for the Study of the Liver (EASL) and the American Association for the Study of Liver Diseases (AASLD) [5] a nodule larger than 2 cm that displays a typical vascular pattern on contrast-enhanced CT or contrast-enhanced MRI can be considered HCC without biopsy. For nodules measuring between 1 and 2 cm, the diagnosis of HCC without biopsy requires a confirmation of the typical vascular pattern on both imaging modalities. In comparison with EASL and AASLD criteria, the consensus statement from the Asian Oncology Summit from 2009 [6] recommends that for any nodule, regardless of size, the characteristic features on contrast-enhanced CT or contrast-enhanced MRI will suffice for a diagnosis of HCC, and obviates the need for biopsy.

The imaging criteria used in these recommendations are based exclusively on the vascular findings of HCC after extracellular contrast agents' administration. A typical enhancement is defined as an early arterial uptake followed by washout in the portovenous or late, equilibrium phase. Moreover, the evaluation of the morphological appearance on unenhanced images together with the evaluation of the vascular features on dynamic contrast-enhanced images enables the radiologist to provide additional information regarding the biomolecular angiogenetic activities in HCCs [7]. On the other hand, there are several limitations to the assessment of HCC using only the vascular criteria. The enhancement pattern of small HCC depends on size and cellular differentiation and HCCs smaller than 2 cm may

Received: 05.04.2011 Accepted: 11.05.2011
J Gastrointestin Liver Dis
June 2011 Vol. 20 No 2, 181-189
Address for correspondence: Nicolae Bolog, MD, MS, PhD
Phoenix Diagnostic Clinic
35 Luigi Cazzavillan, Sector 1
010784 Bucharest, Romania
Email: nbolog@cdphoenix.ro

have atypical enhancement. Moreover, the diagnosis of HCC based on vascular pattern may overlook the hypovascular tumors. Conversely, 52% of small early arterial-enhancing lesions decrease in time and can be considered pseudolesions [8]. The use of tissue-specific contrast agents, including superparamagnetic iron oxides and hepatobiliary contrast agents, improves lesion detection and characterization due to additional cellular information regarding liver tumors including HCC. Therefore, an accurate diagnosis of HCC implies, at this moment, a combination of both, vascular and cellular, information.

This article focuses on the most important findings provided by unenhanced and dynamic-enhanced CT and MR images regarding HCC evaluation. The various imaging characteristics of HCC at MR imaging after the administration of tissue specific contrast agents are also discussed.

Unenhanced and dynamic-enhanced CT and MR imaging

Imaging findings and diagnosis performance

Dynamic contrast-enhanced CT and MRI are widely used for HCC diagnosis and staging. The standard protocol consists of acquisition during separate breath-holds of unenhanced images followed by acquisition of arterial, portovenous, and equilibrium or late phase. MRI is superior to CT in providing structural information on unenhanced images. Different MRI sequences are used to obtain information regarding the liver parenchyma and lesion morphology. The common description on unenhanced MR images refers to HCC as a hypointense lesion on T1-weighted images and hyperintense lesion on T2-weighted images compared to liver parenchyma [9-11]. However, several studies have shown that a more variable appearance of HCC is relatively common [12-14]. Up to 30% of HCC nodules can be isointense on T2-weighted images and 12% to 50% can display hyperintense signal on T1-weighted images [12, 13]. These signal intensity variations on unenhanced images are explained by the presence, in different proportions, of fat, copper, iron, protein, and glycogen within the nodules [15, 16].

Diffusion-weighted MRI has been recently proposed as an additional unenhanced MRI sequence for the evaluation of HCC. Diffusion-weighted MRI is very sensitive to the motion of water protons at the microscopic level in response to thermal energy. Liver tumors appear as high signal intensity lesions in contrast to the low signal intensity of the liver parenchyma [17]. However, the qualitative analysis of the signal intensity on diffusion-weighted images does not enable the differentiation between malignant and benign lesions. A more accurate characterization of focal liver lesions implies a quantitative assessment based on the apparent diffusion coefficient (ADC). By using this quantitative criteria malignant lesions can be differentiated from benign liver lesions based on the lower ADC values on diffusion-weighted images [18, 19]. Several authors [20, 21] have demonstrated that diffusion-weighted MRI enables a better detection of small metastases in contrast with unenhanced T2-weighted images. Another study [17] has shown that the addition of diffusion-weighted imaging to the routine liver MRI in patients with cancer increases the number of the detected metastases with 40%. However, in patients with cirrhosis, HCC may be difficult to differentiate from dysplastic nodules or even from surrounding fibrotic parenchyma [18, 22-24]. A recent study showed that diffusion-weighted imaging has a lower sensitivity (60.7%) for the detection of local HCC recurrence after transarterial chemoembolization (TACE) compared to contrast-enhanced imaging (82%) [25]. In our department, diffusion-weighted MR imaging is part of the routine liver protocol in all patients. We consider that the diffusion images help to detect suspicious small areas within the liver. However, the diffusion images should be interpreted in conjunction with T1 and T2-weighted unenhanced images and contrast-enhanced images [26].

The dynamic-enhanced acquisitions after the administration of extracellular contrast agents help to detect and further characterize HCC. The extracellular contrast agents distribute from the intravascular space into the interstitial space. A typical enhancement is defined as an early arterial uptake followed by washout in the portovenous or delayed phases. Regardless of the imaging technique, the enhancement pattern depends on several morphological characteristics of the lesion, such as vascularity, and leakiness of the vascular endothelial cells [27]. The arterial phase is the most important set of images. HCC is by definition a tumor with high arterial vascularization. During the arterial phase the HCC nodule displays a strong contrast uptake in contrast with the low enhancement of the liver parenchyma (Fig. 1). The liver parenchyma enhances progressively having the maximum uptake in the portovenous and equilibrium phases. During these phases, HCC displays a wash-out of the contrast agent. In Table I, different studies are presented in which the performance of dynamic-enhanced CT and MRI in diagnosing HCC has been verified against histological findings as a standard of reference. The wide range of the sensitivity for both techniques may be explained by differences in patient selection, differences of the contrast agents properties or by variations in the imaging protocol. Pooled estimates of sensitivities of dynamic-enhanced CT and MR imaging for the detection of HCC are 37% and 55%, respectively [28, 29]. The diagnosis of small HCCs is particularly difficult because they have to be differentiated from regenerative nodules, from small hemangiomas, or from arterioportal shunts. All of these benign lesions can display strong arterial uptake. Shimizu et al [8] have demonstrated that a significant percentage of the small early arterial enhancing lesions in patients with cirrhosis or chronic hepatitis are not HCCs. From 104 small arterial-enhancing lesions (< 20 mm) that were round or oval in shape only 28% were classified as HCC based on their interval growth or pathologic confirmation. More than half of the lesions (52%) were considered definitely not HCC and 20% of the

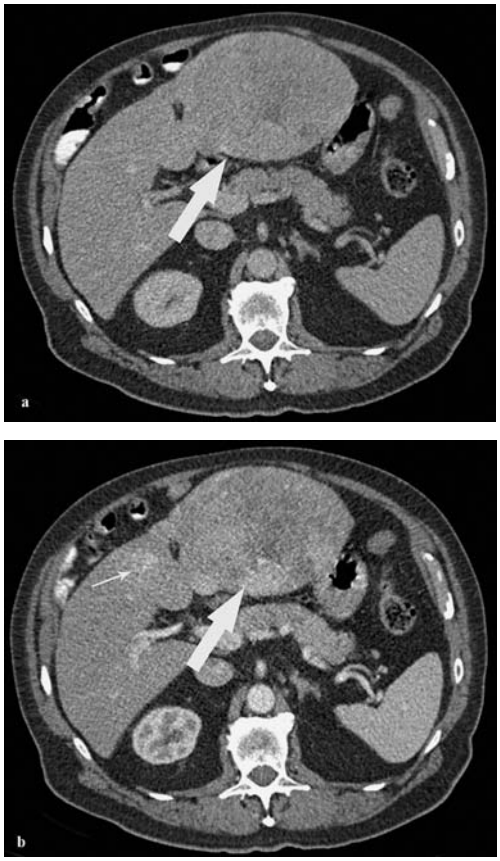

Fig 1. Two HCC nodules in a 58-year-old cirrhotic man. Dynamic-enhanced CT. (a) Axial unenhanced CT image demonstrates a well delineated inhomogenenous nodule in the left lobe (arrow). (b) On an arterial-enhanced CT image the nodule evidences an inhomogeneous enhancement (arrow). Another adjacent hypervascularized nodule is detected (small arrow).

lesions were stable in size and appearance and they were considered probably pseudolesions. Moreover, in their study, 48% of the small HCCs were only detected in the arterial phase and these nodules did not display the typical wash-out pattern in the portal and delayed phases.

The low sensitivity of dynamic-enhanced CT and MRI in diagnosing small nodules of HCC is explained also by the difficulty in the detection and characterization of the nodules with atypical enhancement. Several studies [27, 30-32] have demonstrated that 27% to 34% of the small HCCs are hypovascular. Therefore, the actual criteria based only on the "typical" vascular enhancement pattern should be reconsidered especially in the cases of HCCs smaller than 20 mm.

Correlations of the CT and MRI findings with the biomolecular angiogenetic activities

Recently, the predictions of tumor growth and the relations between imaging findings and biomolecular angiogenetic activities in HCC have been investigated [33-36]. Investigations of these relationships may help radiologists to understand findings related to molecular biologic treatments. The vascular endothelial growth factor (VEGF) is a heparin-binding glycoprotein that is secreted as a homodimer of 45 kd [37]. Solid tumors are composed from vascular and connective stroma and the malignant cells which are dispersed between stroma. The connective tissue provides the vascular supply of the tumor. VEGF plays an important role in regulating angiogenesis, endothelial cell proliferation, and hyperpermeability, and is responsible for the fibrin deposition in tumor [38]. In a study of Suzuki et al [34], it was demonstrated that VEGF is overexpressed in HCC compared with the nontumoral part of the liver. Several studies [34-36, 39] have shown that theVEGF expression in HCC is correlated with several imaging findings. Thus, the more heterogeneous signal intensity of HCC is the stronger VEGF expression of HCC [7]. Heterogeneity of HCC on unenhanced and contrast-enhanced CT and MRI is the result of an uneven distribution of extracellular free water, the presence of fibrosis, fat, and intratumoral necrosis [7]. Rapid cell proliferation in the center of a tumor leads to increased interstitial pressure, which may further lead to compression of vessels, hypoxia, and intratumoral necrosis. An inefficient vascular supply with concomitant hypoxia determines tumor neovascularization to satisfy the needs of tissue [34, 39]. The nonparenchymal and parenchymal hypoxic regions of solid tumors produce powerful and directly angiogenic proteins such as VEGF [39]. Therefore the VEGF expression in the tumor cells seems to be elevated in areas adjacent to tumor necrosis [7, 34]. The presence of fat within HCC is another cause of signal heterogeneity on CT and MR images. It has been shown that hypoxia induces also a higher content of fat within the endothelial cells [40].

Some authors have found a correlation between the VEGF expression and stroma formation [34, 41]. Tumor cells are not known to synthesize fibrinogen. VEGF transcript expression is thought to be responsible for fibrin deposition in the tumor as a result of vascular hyperpermeability [38]. Suzuki et al [34] have demonstrated a statistically significant correlation between VEGF expression and fibrous capsule and septal formation of the tumor. However, it seems that the distribution of fibrotic changes may be determined by VEGF receptors expression, not by VEGF expression [34].

There is data [36] that suggests that VEGF may be a pathophysiological factor that regulates contrast enhancement on dynamic contrast-enhanced imaging studies, and that the expression of VEGF may be estimated with MRI and CT. However, there are controversial reports regarding the correlation between the arterial enhancement of HCC and VEGF expression. Some authors reported that VEGF activity is not correlated with the vascularity of HCCs as determined by conventional angiography [33, 34]. Other authors have reported that VEGF activity correlates directly with the intensity of tumor enhancement on angiography [42]. Kanematsu et al [35] evaluated 20 HCC nodules by using CT angiography and they compared the arterial enhancement with the intensity of VEGF expression in HCC and the surrounding parenchyma. Their results indicated that the more hypervascular an HCC is on CT arterial phase images, the weaker the VEGF expression in the tumor is.

Table I. The reported sensitivities and specificities of dynamic-enhanced CT and MRI with extracellular contrast agents in diagnosing HCC against histological findings as a standard of reference.

Author/year	Imaging technique	HCC mean diameter (mm)	Sensitivity (%)	Specificity (%)
Lim et al / 2000 [83]	Dynamic CT	19	71	
Krinsky et al / 2001 [28]	Dynamic MRI	18	55	
Tomemori et al / 2001 [82]	Dynamic CT	< 20	67.6	
	Dynamic CT	< 20	85.3	
Rode et al / 2001 [72]	Dynamic CT	> 8	53.8	
	Dynamic MRI	> 8	76.9	
Krinsky et al / 2002 [81]	Dynamic MRI	> 20	100	
		10-20	52	
		< 10	4	
Burrel et al / 2003 [73]	MR angiography	29 mm for main nodules and 11 mm for additional nodules	76	
	Dynamic CT		61	
Brancatelli et al / 2003 [80]	Dynamic CT		60.8	52
Valls et al / 2004 [74]	Dynamic CT	> 20	93.6	
		< 20	61	
Kim et al / 2005 [52]	Dynamic CT	> 10	91.3	95.3
		< 10	29	
	Dynamic MRI	> 10	90.2	97
			29	
Kim et al / 2006 [75]	Dynamic CT	18	77.4 - 79.2	
		< 10	47.1	
Ronzoni et al / 2007 [79]	Dynamic CT	17	77	75
Lauenstein et al / 2007 [76]	Dynamic MRI	< 20	35.71	
Forner et al / 2008 [78]	Dynamic MRI	< 20	61.7	96.6
Heilmaier et al / 2009 [27]	Dynamic MRI			
Marin et al / 2009 [77]	Dynamic CT	23	61	
	Dynamic MRI	23	63	

The authors suggested that an increased VEGF expression is present only in HCCs that are hypovascular in arterial phase. A possible cause of the decrease activity of VEGF in hypervascular HCCs is represented by the fact that there is an upregulation of VEGF that leads to gene suppression once a hypervascular HCC has been developed. According to another study [7], there is an inverse correlation between the enhancement intensity of HCCs in the arterial phase on MR images and VEGF activity of the HCC compared to VEGF of the surrounding liver. These results also suggest that the hypervascular HCCs have a low VEGF activity. However, Kwak et al [36] showed that the degree of VEGF expression is directly correlated with the degree of contrast enhancement on arterial-enhanced CT images. The authors suggested that the strong arterial enhancement of HCC is the result of a strong VEGF expression which is responsible for an increased vascular permeability and increased proliferation of the endothelial cells. Further studies are needed to clarify the correlation between the hypo- and hypervascular HCCs in the arterial phase and the expression of VEGF. This correlation may be an important observation when deciding to use the recently developed antiangiogenic tumor therapy involving the use of monoclonal antibody against VEGF.

Tissue specific contrast-enhanced MR imaging

The enhancement patterns at CT and MRI during the different vascular phases after extracellular contrast agents administration is an important tool in the detection and characterization of HCC because many of these lesions are occult on unenhanced images. However, there is general agreement that the diagnostic performance of HCC on dynamic contrast enhanced CT and MR imaging depends on the tumor size with sensitivity and specificity values significantly higher for lesions larger than 20 mm in diameter compared with those smaller than 20 mm. The tissue specific contrast agents were introduced in order to improve the diagnostic accuracy of the liver lesions by targeting different cellular component of the focal liver lesions, such as Kupffer cells or hepatocytes. There are two different types of tissue specific contrast agents that can be used in clinical practice: reticuloendothelial and hepatobiliary contrast agents. By

using these contrast agents the diagnosis of HCC is based on a combination of different imaging features.

Reticuloendothelial contrast agents

The reticuloendothelial contrast agents are taken up by the reticuloendothelial cells particularly from the liver and spleen and reflect the number of functioning Kupffer cells [43]. There are two different types of contrast agents in clinical use and both contain iron-based particles with 30-150 nm in diameter. They are referred to as super paramagnetic iron oxides (SPIO) [44]. Ferumoxides (Feridex, Advanced Magnetics, Cambridge, Mass; Endorem, Guerbet, Aulnay sous Bois, France) are administered as a slow infusion over 30-60 minutes and the imaging is typically performed 1-4 hours after infusion. Ferucarbotran (Resovist; Schering Diagnostics, Berlin, Germany) is administered in bolus and the imaging is performed 10-20 minutes after administration [27, 45-47]. SPIO are used as a negative MR contrast agent. Although SPIO shorten both T1 and T2 relaxation time, in the accumulation phase when the SPIO particles are taken up by the Kupffer cells, T2 and T2* effects and, less frequently T1 effects, are used in lesion detection and characterization. Their superparamagnetic properties determine a reduced signal intensity on T2-weighted images [43]. Tissues with decreased reticuloendothelial system function (i.e., the absence of the Kupffer cells or a low phagocytic activity of the Kupffer cells, such as occurs in metastases and HCC) retain their native signal intensity on T2-weighted images and become more conspicuous in contrast with the lower signal intensity of the normal liver parenchyma (Fig. 2).

Several authors [48, 49] have compared the diagnostic performance of dynamic-enhanced MRI with extracellular contrast agents with SPIO-enhanced MRI for HCC. Some studies [48, 50] showed that SPIO-enhanced T2-weighted images are more accurate than unenhanced and conventional contrast-enhanced CT and MR images. Other studies [47, 49, 51-55] have reported either no significant difference between the two modalities or slightly better performance of contrast-enhanced CT and MR images with extracellular contrast agents. However, there is substantial variability in the number and functionality of Kupffer cells between well-differentiated HCC with almost normal Kupffer cell function and nondifferentiated HCC with depleted Kupffer cells. Therefore, the use of SPIO as a single contrast agent is controversial [46, 48, 49, 51, 54].

The administration of SPIO in conjunction with extracellular contrast agents in the same patient during one MR imaging examination, the so-called double-contrast MR imaging technique, has been proposed in order to overcome the limitations of single-contrast MR imaging in diagnosing HCC [27, 56-59]. Well-differentiated HCC may show some uptake of superparamagnetic iron oxide, and some lesions may mimic the hypervascular features of HCC. Moreover, there are HCCs that are hypovascular and are not detected on dynamic-enhanced imaging. Combining the MR imaging criteria of HCC with both superparamagnetic iron oxide and extracellular contrast agent provides a more rigorous approach to lesion characterization (Table II). On double-contrast MR imaging the differential diagnosis of HCC and other lesions (i.e. hemangiomas, arterioportal shunts, regenerative nodule, dysplastic nodules) is facilitated by the different available information: cellular and vascular. The disadvantages of the use of two contrast agents in one patient consists of the increase in the overall cost of the MR examination and the lengthening of the time for image acquisition and analysis.

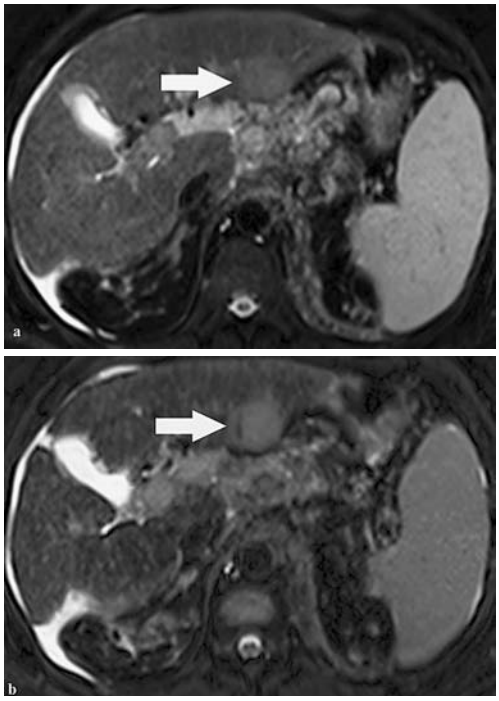

Fig 2. Hepatocellular carcinoma in a 64-year-old cirrhotic man. MR imaging with ferucarbotran. Axial unenhanced T2-weighted image (a) demonstrates a slightly hyperintense nodule (arrow). T2-weighted fat-supressed image obtained 10 minutes after ferucarbotran administration (b) shows increased signal intensity compared to the surrounding liver parenchyma (arrow). A diagnosis of HCC was confirmed at histopathology.

Table II. Criteria for diagnosing HCC at mono-contrast and double-contrast MR imaging techniques [47]

MR Technique	Enhancement pattern of HCC
Mono-contrast dynamic-enhanced with extracellular contrast agents	Hypervascular in arterial phase with wash-out in the portovenous or late phase
Mono-contrast with SPIO-enhanced	Nodules hypointense on unenhaced T2-weighted images which display hyperintensity on T2-weighted images after SPIO administration OR Nodules hyperintense or isointense on unenhanced T2-weighted images with no signal reduction after SPIO administration
Double-Contrast MR imaging	Nodules assessed as HCC on dynamic-enhanced MR imaging with extracellular contrast agents OR on SPIO-enhanced images

Double-contrast MR imaging is highly sensitive for diagnosing HCC in patients with cirrhotic liver. For the detection of HCCs measuring 10-20 mm the reported sensitivity of double-contrast MR imaging is 92% [45, 60]. Several studies have compared double-contrast MR imaging with mono-contrast technique and showed that double-contrast technique significantly improves the diagnosis of HCC [27, 58, 61, 62]. The sequential administration of both types of contrast agents have demonstrated their superiority to the mono-contrast techniques in the assessment of the efficacy of HCC after treatment (i.e. transarterial chemoembolization - TACE) [47]. With the dynamic gadolinium-enhanced technique, the sensitivity, specificity, and accuracy is 68%, 100%, and 72% respectively for viable tumor detection after treatment. The SPIO-enhanced technique is more sensitive (80%) and accurate (83%) compared to the extracellular contrast-enhanced technique (68% sensitivity and 72% accuracy), and the double-contrast technique is more accurate (92%) in viable tumor detection after TACE compared to the mono-contrast techniques [47]. Moreover, it has been demonstrated that the double-contrast technique increases the diagnostic confidence of the radiologist in HCC diagnosis compared with SPIO-enhanced and dynamic-enhanced MR imaging with extracellular contrast agents [27].

Hepatobiliary contrast agents

There are two different MR imaging contrast agents with hepatocyte-selective properties that include the manganese-based and the gadolinium-based [63]. Both contrast agents are considered positive MR imaging agents having a T1-shortening effect. The manganese-based contrast agents (Mn-DPDP, GE Healthcare, Oslo, Norway) are administered as a slow infusion over 10-20 minutes and delayed T1-weighted imaging can be performed 30 minutes to 4 hours after infusion. The gadolinium-based contrast agents (Gd-EOB-DTPA, Bayer-Schering Pharma, Berlin, Germany and Gd-BOPTA, Bracco, Milan, Italy) have double properties. They can be administered in rapid bolus having the same perfusion properties as extracellular contrast agents [63]. After 20 minutes the contrast agent is taken up by the normal hepatocytes and delayed T1-weighted MR images are obtained. Because an important percentage of the contrast agent (i.e. up to 25% for Gd-Bopta and up to 50% for Gd-EOB-DTPA) is excreted through the bile, the biliary tract presents a high degree of enhancement at T1-weighted delayed MR images. This delayed phase is known in MR imaging as the hepatobiliary phase. The hepatobiliary contrast agents are not taken up only by normal liver parenchyma but also by focal liver lesions of hepatocellular origin (adenoma, focal nodular hyperplasia, regenerative and dysplatic nodules in cirrhosis, HCC). Thus, the use of these contrast agents particularly enables the differentiation between hepatocyte-containing from non-hepatocyte-containing lesions (metastases, hepatic cysts, hemangiomas, abscesses) [64]. Many authors have demonstrated that hepatobiliary contrast-enhanced MR imaging is superior to extracellular contrast-enhanced MR imaging and dynamic-enhanced CT in the diagnosis of metastases [65-67]. Moreover, there is data that shows that the total diagnostic cost for the imaging strategy with initial MR imaging with Gd-EOB-DTPA is similar to dynamic-enhanced CT as an initial diagnostic modality, and offers lower costs than dynamic-enhanced MR imaging with extracellular contrast agents in patients with suspected colorectal liver metastases [65]. However, for these patients, MR imaging with hepatobiliary contrast agents improves preoperative planning, and leads to cost savings through shorter operative time and a higher rate of avoidance of unnecessary procedures [65].

In HCC, the degree of enhancement in the hepatobiliary phase is correlated with the degree of differentiation and several authors have based their approach to grading HCC with hepatobiliary uptake in MR imaging [68-70]. The well-differentiated HCCs take up hepatobiliary contrast agents. Therefore, they appear either iso- or hyperintense to liver parenchyma in the hepatobiliary phase. In cirrhotic patients HCC nodules are difficult to be differentiated from the isointense regenerative nodules or hyperintense premalignant dysplastic nodules. The moderately to poorly differentiated HCCs do not display hepatobiliary contrast agent uptake and they appear hypointense at MR imaging in the hepatobilary phase (Fig 3). The overall pooled sensitivity for detection of HCC at liver imaging with hepatobiliary contrast agents is 81% [71]. Some authors [71] have proposed that the use of hepatobiliary contrast agents in cirrhotic patients should be reserved for problematic cases in order to determine the degree of differentiation of HCC. However, the perfusion properties of the gadolinium-based hepatobiliary contrast agents enables a bimodal evaluation of HCCs based on both a vascular and hepatobiliary pattern (Table III).

Table III. Vascular and hepatobiliary criteria for diagnosing HCC at MR imaging with gadolinium-based hepatobiliary contrast agents.

Enhancement pattern of HCC	
Typical vascular pattern of the nodule on dynamic-enhanced images[1]	Atypical vascular pattern of the nodule[2] AND Hypointense nodule compared to liver parenchyma on hepatobiliary phase images[3]

Notes
1. A typical vascular pattern is defined as an early arterial uptake followed by washout in the portovenous or equilibrium phases;
2. An atypical vascular pattern is defined as any pattern that differ from the typical enhancement in any of the vascular phases (ie. hypo- or -isointense on arterial phase with no washout in later phases);
3. The hypointensity of the nodule in the hepatobiliary phase is an indicator of the presence of a moderately to poorly differentiated HCC.

Conclusion

The final diagnosis of HCC is increasingly based on imaging criteria. The evaluation of the dynamic-enhanced CT and MR images provides valuable information regarding the vascular pattern and additional information regarding the biomolecular angiogenetic activities in HCCs. However, there are several limitations of the vascular evaluation

Fig 3. Hepatocellular carcinoma in a 49-year-old woman. Dynamic-enhanced MR imaging and hepatobiliary phase MR imaging with Gd-EOB-DTPA. Axial unenhanced T1-weighted image (a) demonstrates a small hypointense subcaspular nodule (arrow). Axial T1-weighted fat-suppressed image (b) acquired in the hepatobiliary phase 20 minutes after Gd-EOB-DTPA administration shows that the lesion (arrow) demonstrates no uptake of Gd-EOB-DTPA. Surgical resection yielded HCC. Note concomitant excretion of Gd-EOB-DTPA in the biliary tree (small arrow in b).

of HCC. The administration of the cellular specific MR imaging contrast agents may overcome these limitations in diagnosing HCC.

Conflicts of interest

None to declare.

References

1. Willatt JM, Hussain HK, Adusumilli S, Marrero JA. MR Imaging of hepatocellular carcinoma in the cirrhotic liver: challenges and controversies. Radiology 2008; 247:311-330.
2. Parkin DM, Bray FI, Devesa SS. Cancer burden in the year 2000. The global picture. Eur J Cancer 2001; 37 Suppl 8:S4-66.
3. Llovet JM, Schwartz M, Mazzaferro V. Resection and liver transplantation for hepatocellular carcinoma. Semin Liver Dis 2005; 25:181-200.
4. Colli A, Fraquelli M, Conte D. Alpha-fetoprotein and hepatocellular carcinoma. Am J Gastroenterol 2006; 101:1939; author reply 1940-1941.
5. Bruix J, Sherman M. Management of hepatocellular carcinoma. Hepatology 2005; 42:1208-1236.
6. Poon D, Anderson BO, Chen LT, et al. Management of hepatocellular carcinoma in Asia: consensus statement from the Asian Oncology Summit 2009. Lancet Oncol 2009; 10:1111-1118.
7. Kanematsu M, Osada S, Amaoka N, et al. Expression of vascular endothelial growth factor in hepatocellular carcinoma and the surrounding liver and correlation with MRI findings. AJR Am J Roentgenol 2005; 184:832-841.
8. Shimizu A, Ito K, Koike S, Fujita T, Shimizu K, Matsunaga N. Cirrhosis or chronic hepatitis: evaluation of small (<or=2-cm) early-enhancing hepatic lesions with serial contrast-enhanced dynamic MR imaging. Radiology 2003; 226:550-555.
9. Rummeny E, Saini S, Wittenberg J, et al. MR imaging of liver neoplasms. AJR Am J Roentgenol 1989; 152:493-499.
10. Kadoya M, Matsui O, Takashima T, Nonomura A. Hepatocellular carcinoma: correlation of MR imaging and histopathologic findings. Radiology 1992; 183:819-825.
11. Yamashita Y, Fan ZM, Yamamoto H, et al. Spin-echo and dynamic gadolinium-enhanced FLASH MR imaging of hepatocellular carcinoma: correlation with histopathologic findings. J Magn Reson Imaging 1994; 4:83-90.
12. Kelekis NL, Semelka RC, Worawattanakul S, et al. Hepatocellular carcinoma in North America: a multiinstitutional study of appearance on T1-weighted, T2-weighted, and serial gadolinium-enhanced gradient-echo images. AJR Am J Roentgenol 1998; 170:1005-1013.
13. Mahfouz AE, Hamm B, Taupitz M, Wolf KJ. Hypervascular liver lesions: differentiation of focal nodular hyperplasia from malignant tumors with dynamic gadolinium-enhanced MR imaging. Radiology 1993; 186:133-138.
14. Itoh K, Nishimura K, Togashi K, et al. Hepatocellular carcinoma: MR imaging. Radiology 1987; 164:21-25.
15. Mitchell DG, Kim I, Chang TS, et al. Fatty liver. Chemical shift phase-difference and suppression magnetic resonance imaging techniques in animals, phantoms, and humans. Invest Radiol 1991; 26:1041-1052.
16. Ebara M, Watanabe S, Kita K, et al. MR imaging of small hepatocellular carcinoma: effect of intratumoral copper content on signal intensity. Radiology 1991; 180:617-621.
17. Low RN, Gurney J. Diffusion-weighted MRI (DWI) in the oncology patient: value of breathhold DWI compared to unenhanced and gadolinium-enhanced MRI. J Magn Reson Imaging 2007; 25:848-858.
18. Taouli B, Vilgrain V, Dumont E, Daire JL, Fan B, Menu Y. Evaluation of liver diffusion isotropy and characterization of focal hepatic lesions with two single-shot echo-planar MR imaging sequences: prospective study in 66 patients. Radiology 2003; 226:71-78.
19. Namimoto T, Yamashita Y, Sumi S, Tang Y, Takahashi M. Focal liver masses: characterization with diffusion-weighted echo-planar MR imaging. Radiology 1997; 204:739-744.
20. Zech CJ, Herrmann KA, Dietrich O, Horger W, Reiser MF, Schoenberg SO. Black-blood diffusion-weighted EPI acquisition of the liver with parallel imaging: comparison with a standard T2-weighted sequence for detection of focal liver lesions. Invest Radiol 2008; 43:261-266.
21. Parikh T, Drew SJ, Lee VS, et al. Focal liver lesion detection and characterization with diffusion-weighted MR imaging: comparison with standard breath-hold T2-weighted imaging. Radiology 2008; 246:812-822.
22. Yamada I, Aung W, Himeno Y, Nakagawa T, Shibuya H. Diffusion

coefficients in abdominal organs and hepatic lesions: evaluation with intravoxel incoherent motion echo-planar MR imaging. Radiology 1999; 210:617-623.
23. Vossen JA, Buijs M, Liapi E, Eng J, Bluemke DA, Kamel IR. Receiver operating characteristic analysis of diffusion-weighted magnetic resonance imaging in differentiating hepatic hemangioma from other hypervascular liver lesions. J Comput Assist Tomogr 2008; 32:750-756.
24. Goshima S, Kanematsu M, Kondo H, et al. Diffusion-weighted imaging of the liver: optimizing b value for the detection and characterization of benign and malignant hepatic lesions. J Magn Reson Imaging 2008; 28:691-697.
25. Goshima S, Kanematsu M, Kondo H, et al. Evaluating local hepatocellular carcinoma recurrence post-transcatheter arterial chemoembolization: is diffusion-weighted MRI reliable as an indicator? J Magn Reson Imaging 2008; 27:834-839.
26. Taouli B, Koh DM. Diffusion-weighted MR imaging of the liver. Radiology 2010; 254:47-66.
27. Heilmaier C, Lutz AM, Bolog N, Weishaupt D, Seifert B, Willmann JK. Focal liver lesions: detection and characterization at double-contrast liver MR Imaging with ferucarbotran and gadobutrol versus single-contrast liver MR imaging. Radiology 2009; 253:724-733.
28. Krinsky GA, Lee VS, Theise ND, et al. Hepatocellular carcinoma and dysplastic nodules in patients with cirrhosis: prospective diagnosis with MR imaging and explantation correlation. Radiology 2001; 219:445-454.
29. Peterson MS, Baron RL, Marsh JW, Jr., Oliver JH, 3rd, Confer SR, Hunt LE. Pretransplantation surveillance for possible hepatocellular carcinoma in patients with cirrhosis: epidemiology and CT-based tumor detection rate in 430 cases with surgical pathologic correlation. Radiology 2000; 217:743-749.
30. Kudo M. Imaging diagnosis of hepatocellular carcinoma and premalignant/borderline lesions. Semin Liver Dis 1999; 19:297-309.
31. Hayashi M, Matsui O, Ueda K, Kawamori Y, Gabata T, Kadoya M. Progression to hypervascular hepatocellular carcinoma: correlation with intranodular blood supply evaluated with CT during intraarterial injection of contrast material. Radiology 2002; 225:143-149.
32. Bolondi L, Gaiani S, Celli N, et al. Characterization of small nodules in cirrhosis by assessment of vascularity: the problem of hypovascular hepatocellular carcinoma. Hepatology 2005; 42:27-34.
33. El-Assal ON, Yamanoi A, Soda Y, et al. Clinical significance of microvessel density and vascular endothelial growth factor expression in hepatocellular carcinoma and surrounding liver: possible involvement of vascular endothelial growth factor in the angiogenesis of cirrhotic liver. Hepatology 1998; 27:1554-1562.
34. Suzuki K, Hayashi N, Miyamoto Y, et al. Expression of vascular permeability factor/vascular endothelial growth factor in human hepatocellular carcinoma. Cancer Res 1996; 56:3004-3009.
35. Kanematsu M, Osada S, Amaoka N, et al. Expression of vascular endothelial growth factor in hepatocellular carcinoma and the surrounding liver: correlation with angiographically assisted CT. AJR Am J Roentgenol 2004; 183:1585-1593.
36. Kwak BK, Shim HJ, Park ES, et al. Hepatocellular carcinoma: correlation between vascular endothelial growth factor level and degree of enhancement by multiphase contrast-enhanced computed tomography. Invest Radiol 2001; 36:487-492.
37. Houck KA, Leung DW, Rowland AM, Winer J, Ferrara N. Dual regulation of vascular endothelial growth factor bioavailability by genetic and proteolytic mechanisms. J Biol Chem 1992; 267:26031-26037.
38. Senger DR, Van de Water L, Brown LF, et al. Vascular permeability factor (VPF, VEGF) in tumor biology. Cancer Metastasis Rev 1993; 12:303-324.
39. von Marschall Z, Cramer T, Hocker M, Finkenzeller G, Wiedenmann B, Rosewicz S. Dual mechanism of vascular endothelial growth factor upregulation by hypoxia in human hepatocellular carcinoma. Gut 2001; 48:87-96.
40. Kutami R, Nakashima Y, Nakashima O, Shiota K, Kojiro M. Pathomorphologic study on the mechanism of fatty change in small hepatocellular carcinoma of humans. J Hepatol 2000; 33:282-289.
41. Brown LF, Berse B, Jackman RW, et al. Expression of vascular permeability factor (vascular endothelial growth factor) and its receptors in breast cancer. Hum Pathol 1995; 26:86-91.
42. Mise M, Arii S, Higashituji H, et al. Clinical significance of vascular endothelial growth factor and basic fibroblast growth factor gene expression in liver tumor. Hepatology 1996; 23:455-464.
43. Ferrucci JT, Stark DD. Iron oxide-enhanced MR imaging of the liver and spleen: review of the first 5 years. AJR Am J Roentgenol 1990; 155:943-950.
44. Sjogren CE, Johansson C, Naevestad A, Sontum PC, Briley-Saebo K, Fahlvik AK. Crystal size and properties of superparamagnetic iron oxide (SPIO) particles. Magn Reson Imaging 1997; 15:55-67.
45. Ward J, Guthrie JA, Scott DJ, et al. Hepatocellular carcinoma in the cirrhotic liver: double-contrast MR imaging for diagnosis. Radiology 2000; 216:154-162.
46. Lutz AM, Willmann JK, Goepfert K, Marincek B, Weishaupt D. Hepatocellular carcinoma in cirrhosis: enhancement patterns at dynamic gadolinium- and superparamagnetic iron oxide-enhanced T1-weighted MR imaging. Radiology 2005; 237:520-528.
47. Bolog N, Pfammatter T, Mullhaupt B, Andreisek G, Weishaupt D. Double-contrast magnetic resonance imaging of hepatocellular carcinoma after transarterial chemoembolization. Abdom Imaging 2008; 33:313-323.
48. Reimer P, Jahnke N, Fiebich M, et al. Hepatic lesion detection and characterization: value of nonenhanced MR imaging, superparamagnetic iron oxide-enhanced MR imaging, and spiral CT-ROC analysis. Radiology 2000; 217:152-158.
49. Vogl TJ, Schwarz W, Blume S, et al. Preoperative evaluation of malignant liver tumors: comparison of unenhanced and SPIO (Resovist)-enhanced MR imaging with biphasic CTAP and intraoperative US. Eur Radiol 2003; 13:262-272.
50. Kang BK, Lim JH, Kim SH, et al. Preoperative depiction of hepatocellular carcinoma: ferumoxides-enhanced MR imaging versus triple-phase helical CT. Radiology 2003; 226:79-85.
51. Simon G, Link TM, Wortler K, et al. Detection of hepatocellular carcinoma: comparison of Gd-DTPA- and ferumoxides-enhanced MR imaging. Eur Radiol 2005; 15:895-903.
52. Kim SH, Choi D, Lim JH, et al. Ferucarbotran-enhanced MRI versus triple-phase MDCT for the preoperative detection of hepatocellular carcinoma. AJR Am J Roentgenol 2005; 184:1069-1076.
53. Ba-Ssalamah A, Heinz-Peer G, Schima W, et al. Detection of focal hepatic lesions: comparison of unenhanced and SHU 555 A-enhanced MR imaging versus biphasic helical CTAP. J Magn Reson Imaging 2000; 11:665-672.
54. Nakamura H, Ito N, Kotake F, Mizokami Y, Matsuoka T. Tumor-detecting capacity and clinical usefulness of SPIO-MRI in patients with hepatocellular carcinoma. J Gastroenterol 2000; 35:849-855.
55. Pauleit D, Textor J, Bachmann R, et al. Hepatocellular carcinoma: detection with gadolinium- and ferumoxides-enhanced MR imaging of the liver. Radiology 2002; 222:73-80.
56. Bolog N LA, Weishaupt D, Willmann J. Double-Contrast MR imaging of the liver: detection and characterization of focal liver lesions In:RSNA Chicago, 2007.
57. Guiu B, Loffroy R, Ben Salem D, et al. Combined SPIO-gadolinium magnetic resonance imaging in cirrhotic patients: negative predictive

value and role in screening for hepatocellular carcinoma. Abdom Imaging 2008; 33:520-528.
58. Hanna RF, Kased N, Kwan SW, et al. Double-contrast MRI for accurate staging of hepatocellular carcinoma in patients with cirrhosis. AJR Am J Roentgenol 2008; 190:47-57.
59. Yoo HJ, Lee JM, Lee MW, et al. Hepatocellular carcinoma in cirrhotic liver: double-contrast-enhanced, high-resolution 3.0T-MR imaging with pathologic correlation. Invest Radiol 2008; 43:538-546.
60. Bhartia B, Ward J, Guthrie JA, Robinson PJ. Hepatocellular carcinoma in cirrhotic livers: double-contrast thin-section MR imaging with pathologic correlation of explanted tissue. AJR Am J Roentgenol 2003; 180:577-584.
61. Guiu B, Loffroy R, Cercueil JP. Double-contrast MRI in patients with cirrhosis. AJR Am J Roentgenol 2008; 191:W78.
62. Kwak HS, Lee JM, Kim CS. Preoperative detection of hepatocellular carcinoma: comparison of combined contrast-enhanced MR imaging and combined CT during arterial portography and CT hepatic arteriography. Eur Radiol 2004; 14:447-457.
63. Ba-Ssalamah A, Uffmann M, Saini S, Bastati N, Herold C, Schima W. Clinical value of MRI liver-specific contrast agents: a tailored examination for a confident non-invasive diagnosis of focal liver lesions. Eur Radiol 2009; 19:342-357.
64. Huppertz A, Haraida S, Kraus A, et al. Enhancement of focal liver lesions at gadoxetic acid-enhanced MR imaging: correlation with histopathologic findings and spiral CT--initial observations. Radiology 2005; 234:468-478.
65. Zech CJ, Grazioli L, Jonas E, et al. Health-economic evaluation of three imaging strategies in patients with suspected colorectal liver metastases: Gd-EOB-DTPA-enhanced MRI vs. extracellular contrast media-enhanced MRI and 3-phase MDCT in Germany, Italy and Sweden. Eur Radiol 2009; 19 Suppl 3:S753-763.
66. Vogl TJ, Kummel S, Hammerstingl R, et al. Liver tumors: comparison of MR imaging with Gd-EOB-DTPA and Gd-DTPA. Radiology 1996; 200:59-67.
67. Huppertz A, Balzer T, Blakeborough A, et al. Improved detection of focal liver lesions at MR imaging: multicenter comparison of gadoxetic acid-enhanced MR images with intraoperative findings. Radiology 2004; 230:266-275.
68. Ni Y, Marchal G, Yu J, Muhler A, Lukito G, Baert AL. Prolonged positive contrast enhancement with Gd-EOB-DTPA in experimental liver tumors: potential value in tissue characterization. J Magn Reson Imaging 1994; 4:355-363.
69. Ni Y, Marchal G. Enhanced magnetic resonance imaging for tissue characterization of liver abnormalities with hepatobiliary contrast agents: an overview of preclinical animal experiments. Top Magn Reson Imaging 1998; 9:183-195.
70. Marchal G, Zhang X, Ni Y, Van Hecke P, Yu J, Baert AL. Comparison between Gd-DTPA, Gd-EOB-DTPA, and Mn-DPDP in induced HCC in rats: a correlation study of MR imaging, microangiography, and histology. Magn Reson Imaging 1993; 11:665-674.
71. Seale MK, Catalano OA, Saini S, Hahn PF, Sahani DV. Hepatobiliary-specific MR contrast agents: role in imaging the liver and biliary tree. Radiographics 2009; 29:1725-1748.
72. Rode A, Bancel B, Douek P, et al. Small nodule detection in cirrhotic livers: evaluation with US, spiral CT, and MRI and correlation with pathologic examination of explanted liver. J Comput Assist Tomogr 2001; 25:327-336.
73. Burrel M, Llovet JM, Ayuso C, et al. MRI angiography is superior to helical CT for detection of HCC prior to liver transplantation: an explant correlation. Hepatology 2003; 38:1034-1042.
74. Valls C, Cos M, Figueras J, et al. Pretransplantation diagnosis and staging of hepatocellular carcinoma in patients with cirrhosis: value of dual-phase helical CT. AJR Am J Roentgenol 2004; 182:1011-1017.
75. Kim YK, Kim CS, Chung GH, et al. Comparison of gadobenate dimeglumine-enhanced dynamic MRI and 16-MDCT for the detection of hepatocellular carcinoma. AJR Am J Roentgenol 2006; 186:149-157.
76. Lauenstein TC, Salman K, Morreira R, et al. Gadolinium-enhanced MRI for tumor surveillance before liver transplantation: center-based experience. AJR Am J Roentgenol 2007; 189:663-670.
77. Marin D, Di Martino M, Guerrisi A, et al. Hepatocellular carcinoma in patients with cirrhosis: qualitative comparison of gadobenate dimeglumine-enhanced MR imaging and multiphasic 64-section CT. Radiology 2009; 251:85-95.
78. Forner A, Vilana R, Ayuso C, et al. Diagnosis of hepatic nodules 20 mm or smaller in cirrhosis: Prospective validation of the noninvasive diagnostic criteria for hepatocellular carcinoma. Hepatology 2008; 47:97-104.
79. Ronzoni A, Artioli D, Scardina R, et al. Role of MDCT in the diagnosis of hepatocellular carcinoma in patients with cirrhosis undergoing orthotopic liver transplantation. AJR Am J Roentgenol 2007; 189:792-798.
80. Brancatelli G, Baron RL, Peterson MS, Marsh W. Helical CT screening for hepatocellular carcinoma in patients with cirrhosis: frequency and causes of false-positive interpretation. AJR Am J Roentgenol 2003; 180:1007-1014.
81. Krinsky GA, Lee VS, Theise ND, et al. Transplantation for hepatocellular carcinoma and cirrhosis: sensitivity of magnetic resonance imaging. Liver Transpl 2002; 8:1156-1164.
82. Tomemori T, Yamakado K, Nakatsuka A, Sakuma H, Matsumura K, Takeda K. Fast 3D dynamic MR imaging of the liver with MR SmartPrep: comparison with helical CT in detecting hypervascular hepatocellular carcinoma. Clin Imaging 2001; 25:355-361.
83. Lim JH, Kim CK, Lee WJ, et al. Detection of hepatocellular carcinomas and dysplastic nodules in cirrhotic livers: accuracy of helical CT in transplant patients. AJR Am J Roentgenol 2000; 175:693-698.